Preparation of $Mg_{55}Ni_{35}Si_{10}$ Amorphous Powders by Mechanical Alloying and Consolidation by Vacuum Hot Pressing

2006 Chinese Phys. Lett. 23 2161

(http://iopscience.iop.org/0256-307X/23/8/055)

Preparation of $Mg_{55}Ni_{35}Si_{10}$ Amorphous Powders by Mechanical Alloying and Consolidation by Vacuum Hot Pressing *

YANG Deng-Ke(杨登科)[1], WEN Cui-E(文翠娥)[2], HAN Fu-Sheng(韩福生),
WANG Qing-Zhou(王清周)[1], LI Hai-Jin(李海金)[1]

[1]*Key Laboratory of Materials Physics, Institute of Solid State Physics, Chinese Academy of Sciences, Hefei 230031*
[2]*School of Engineering and Technology, Deakin University, Geelong Victoria 3217, Australia*

(Received 11 April 2006)

Amorphous $Mg_{55}Ni_{35}Si_{10}$ powders are fabricated by using a mechanical alloying technique. The amorphous powders are found to exhibit a relatively high crystallization temperature of 380° C. The as-milled amorphous $Mg_{55}Ni_{35}Si_{10}$ powders are consolidated successfully into bulk body by vacuum hot pressing technique. Limited nanocrystallization is noticed. The Vickers microhardness range of the $Mg_{55}Ni_{35}Si_{10}$ bulk sample is 7834 to 8048 MPa. Its bending strength and compressive strength are 529 MPa and 1466 MPa, respectively.

PACS: 61. 43. Dq, 81. 05. Zx, 81. 20. Ev

Mg alloys are well-known light-weight alloy systems with outstanding specific mechanical properties that may find applications in a number of engineering fields. Unfortunately, the plasticity and the toughness of Mg alloys are usually unsatisfactory, and implementation treatments have to be conducted to improve these properties. As is widely reported, metallic materials with amorphous phase show extraordinary physical and mechanical properties. This suggests that the plasticity and the toughness of the Mg alloys can be modified by an amorphization way.[1−4] Recently, amorphous powders Mg–Y–Cu,[5,6] Mg–Ni–Ge,[7] Mg–Ni–Sn,[8], Mg–Ni–Y,[9,10] and Mg–Al–Ca[11] have been prepared by mechanical alloying (MA). However, a survey of the available literature indicates that little work has been performed on the consolidation of mechanical alloyed Mg-based amorphous powders, probably because Mg-based amorphous alloys are difficult to consolidate due to their low crystallization temperatures and narrow super cooled liquid regions. It is therefore very interesting to investigate the feasibility of preparing Mg-based bulk amorphous by a hot pressing method. Therefore, in this work, mechanical alloying and hot pressing are performed to fabricate the bulk bodies of $Mg_{55}Ni_{35}Si_{10}$ amorphous. The amorphization mechanism of Mg–Ni–Si powders and the mechanical properties of amorphous $Mg_{55}Ni_{35}Si_{10}$ bulk bodies are also tested.

The starting materials are elemental Mg, Ni and Si powders with the purity of 99.9% and the nominal mean diameters of 180 μm, 35 μm and 44 μm, respectively. The powders were weighed in terms of the targeted composition of $Mg_{55}Ni_{35}Si_{10}$ in atom percent. There are 20 g starting powders and 400 g stainless steel balls (10 mm in diameter) used in each ball milling process. To establish a balance between cold welding and fracturing of agglomerates, 2 wt.% stearic acid was added into the powder mixtures before the milling. The MA was conducted in a Retsch mill (PM400). The rotation speed was 200 rpm and the milling time ranged from 20 to 68 h. The pot was taken into a glove box every 5 h to remove the adherent powders from the pot wall and to break the agglomerated powders. Meanwhile, a small amount of powders were taken out from the pot to examine the evolution of the microstructures of the milled powders. The 68-h as-milled powders were consolidated in a vacuum hot pressing machine to prepare bulk amorphous powders with dimensions $10 \times 5 \times 3\,\mathrm{mm}^3$. The hot pressing was performed at 350° C under a pressure of approximately 400 MPa. The hot pressing chamber was evacuated and the pressure was applied during the whole consolidating process. The milled powders and consolidated samples were characterized by x-ray diffraction (XRD) using Cu K_α radiation (X' Pert Pro MPD); differential scanning calorimetry (DSC, Pyris Diamond) at a heating rate of 20°C/min under argon atmosphere; high resolution transmission electron microscopy (HRTEM, Philips JEM2010) and scanning electron microscopy (SEM, Sirion 200FEG). In addition, the Vickers microhardness of the compacted sample was measured with a Matsuzawa MXT50-UL machine using loads of 200, 300, 500, 800 and 1000 g, respectively. Compressive and bending tests were performed on a computer controlled universal testing machine (CMT4204) at a crosshead speed of 2 mm/min. Its density was measured by the Archimedes method.

Figure 1 shows the typical XRD spectra of the $Mg_{55}Ni_{35}Si_{10}$ alloy powders milled for different times from 20 to 68 h. For the initial mixture of the powders, sharp diffraction peaks related to *hcp*-Mg, *fcc*-Ni and *fcc*-Si appear in the spectrum. These peaks grad-

* Supported by the Natural Science Foundation of Anhui Province under Grant No 050440601.
** To whom correspondence should be addressed. Email: fshan@issp.ac.cn

ually became lower and broader and some peaks even disappeared with increasing milling time, as shown in Figs. 1(b) and 1(c), due to the refinement of the crystalline grains and increase of lattice strain. With further increase of milling time such as 44 h, however, only small Ni peaks can be seen while the Mg and Si related peaks are almost invisible. This phenomenon should not be attributed to the dissolution of Mg and Si in Ni because the Ni diffraction peaks did not shift.[12] In order to understand the state of Mg and Si at this stage, the powders milled for 44 h were analysed by HRTEM, as shown by the bright field image and the diffraction pattern in the inset in Figs. 2(a). It is seen that in addition to the sharp diffraction rings and some bright spots, a diffusive diffraction rings presented near the centre, showing the existence of an amorphous phase. Therefore, most of the Mg and Si and some of Ni in this stage have transformed into amorphous phase in this stage. The broad and smooth peak shown in Fig. 1(e) demonstrates that a single amorphous phase can be achieved after milling for 68 h. Such a complete amorphous phase is confirmed by Figs. 2(b), in which the selected-zone diffraction pattern also shows diffusive ring relating to an amorphous phase.

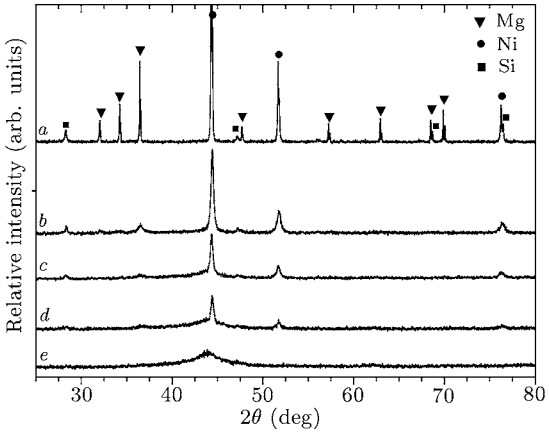

Fig. 1. XRD patterns of $Mg_{55}Ni_{35}Si_{10}$ powders after milling for (a) 0 h, (b) 20 h, (c) 30 h, (d) 44 h, (e) 68 h.

Figure 3 shows the DSC curves of the $Mg_{55}Ni_{35}Si_{10}$ powders milled for 20, 44 and 68 h, illustrating the differences among the three milling times. The powders milled for 20 h exhibit a broad endothermic peak at about 260 μC, while the powders milled for 44 h not only shows a smaller endothermic peak at an elevated temperature, but also exhibits a sharp exothermic peak at around 410 μC. For the powder milled for 68 h, however, only a sharp exothermic peak appears at 420 μC and no endothermic peak can be seen. Since heavy plastic deformation arises during ball milling, very high dislocation population can be produced as a result of the shearing stress generated by the stainless steal balls, as shown in Figs. 2(a). In the corresponding selected zone diffraction pattern depicted in Figs. 2(a), the bright Laue spots suggest that the oriented particles have very fine crystalline grains in the unprocessed Ni powder. In addition, the sharp diffraction rings also demonstrate the occurrence of the amorphous phase. It is in good agreement with the DSC results shown in Fig. 3(b), where the first endothermic peak is caused by the reaction of he unprocessed Mg, Ni and Si powders to form new phases. Increasing milling time leads to decreasing contents of the unprocessed Mg, Ni and Si and thus gives rise to increasing amount of the amorphous phase. Moreover, the enthalpy ΔH of the endothermic peak for the powders milled for 44 h is smaller than that for the powders milled for 20 h, while the enthalpy ΔH of the exothermic peak for the powders milled for 44 h is smaller than that for powders milled for 68 h. These differences are consistent with the crystallization temperatures of the powders undergoing varied milling times and they also disclose the evolution of the microstructures in the amorphous phases.

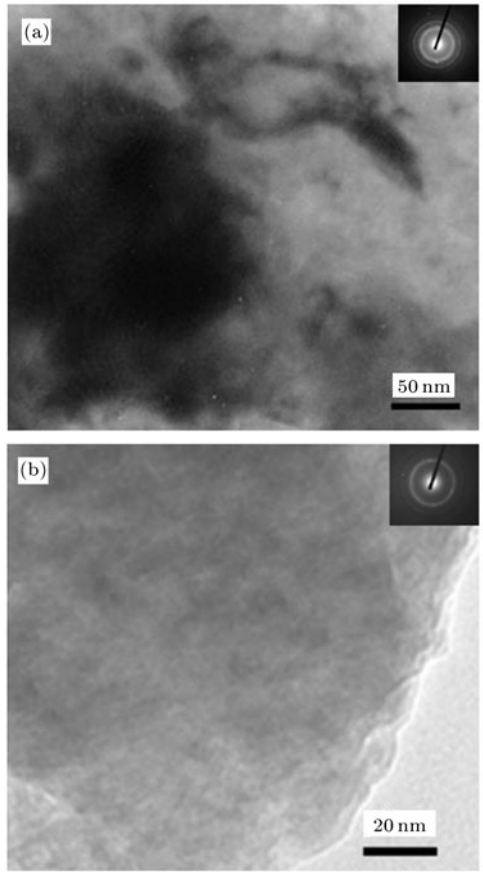

Fig. 2. Bright field image and diffraction pattern (inset) for $Mg_{55}Ni_{35}Si_{10}$ powders after milling for (a) 44 h and (b) 68 h.

From the above analysis, it is concluded that the microstructures of the powders developed in the order of the grain refinement, the formation of the amorphous of Mg and Si and the formation of the amor-

phous $Mg_{55}Ni_{35}Si_{10}$ alloy. This process can be also described by the following reaction:

$$Mg+Ni+Si \rightarrow Mg_{nanocrystalline}+Ni_{nanocrystalline} + Si_{nanocrystalline} \rightarrow (Mg\text{–}Ni\text{–}Si)+Ni_{nanocrystalline} \rightarrow (Mg_{55}Ni_{35}Si_{10})_{amorphous}.$$

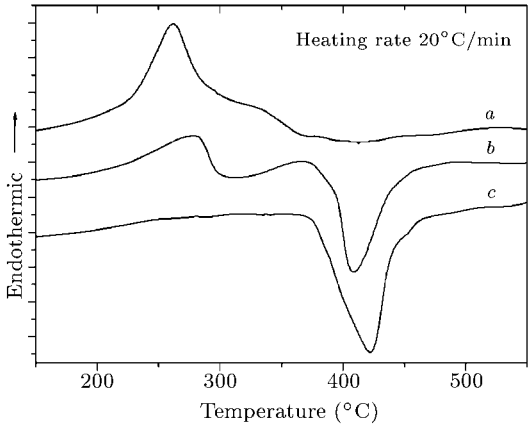

Fig. 3. DSC curves of $Mg_{55}Ni_{35}Si_{10}$ powders after milling for (a) 20 h, (b) 44 h, (c) 68 h.

Based on the DSC results, the 68 h as-milled $Mg_{55}Ni_{35}Si_{10}$ powders were consolidated by vacuum hot pressing technique into bar shape with dimensions $10 \times 5 \times 3\,mm^3$. Powders were hot pressed at 350°C under a pressure of 400 MPa for 5 h. Figure 4 displays the XRD spectrum of the 68 h as-milled powders and the bulk $Mg_{55}Ni_{35}Si_{10}$ specimen. Though the pressing temperature was set at 350°C, which is 30°C below the crystallization temperature, limited nanocrystalline of $MgNi_2$ and Mg_2Ni_5Si phases from the amorphous phase were noticed. It can be noted that the amorphous phase still remains after consolidating at a temperature of 350°C. However, the half maximum line width for the halo pattern of the bulk sample (Fig. 4(b)) is slightly narrower than that of the as-milled powders (Fig. 4(a)). This may be due to strain relief and limited nanocrystallization during consolidating the bulk sample. As shown in Fig. 5, HRTEM observation confirms that some nanoparticles in size 30–50 nm were embed within the amorphous matrix. The selected area diffraction (SAD) pattern of the amorphous matrix presents a typical amorphous phase representing diffusion halo with limited diffraction spots. This implies that the amorphous composite was prepared successfully by hot pressing the as-milled powders at 350°C under a pressure of 400 MPa, only limited nanocrystallization occurred during consolidation.

The presence of the amorphous phase in the consolidated bulk alloy can be further confirmed by DSC scans. Figure 6 shows the DSC scans for the as-milled powders and the hot pressed sample. It can be noted from Fig. 6 that the peak indicating the crystallization temperature of $Mg_{55}Ni_{35}Si_{10}$ samples moves to the left. This may be attributed to the nanocrystallization within the samples and can be identified clearly by the XRD pattern in Fig. 4. These nanocrystallines within the hot pressed samples serve as the nucleation sites during crystallization and induce a decrease of the peak position.

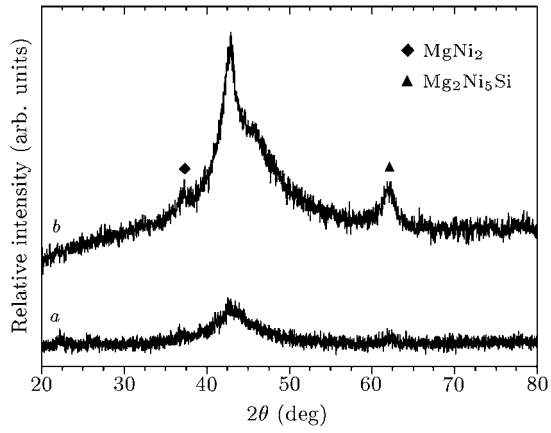

Fig. 4. XRD patterns of $Mg_{55}Ni_{35}Si_{10}$ for (a) the 68-h as-milled and (b) bulk specimens.

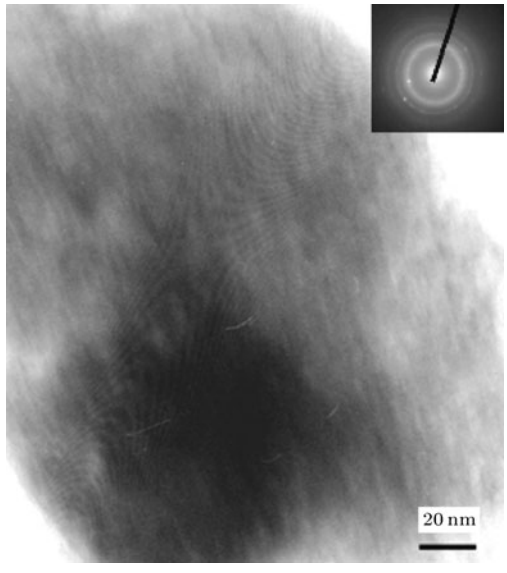

Fig. 5. Bright field image and the diffraction pattern (inset) for bulk $Mg_{55}Ni_{35}Si_{10}$ specimen.

The Vickers microhardnesses of the bulk amorphous samples are presented in Fig. 7. It can be seen that the microhardnesses are ranged from 7834 to 8048 MPa. It is also noted that the microhardness decreases obviously from 8048 to 7900 MPa, when the applied load exceeds 500 g. which is similar to that observed in the conventional crystalline materials, i.e. the apparent hardness always decreases with the increasing applied load.[13] The change in the microhardnesses under different loads may be mainly due to the elastic response during the indentation. The relationship between the applied load and indenta-

tion diagonal length is known as Meyer's law that affects more strongly when the applied load is relatively small.[14] For an ideal indentation test, the microhardness is independent of the applied load or indentation size. However, when the load is small, the indentation size is small and the elastic recovery relative to the indentation size during unloading is large. This may account for the relatively high value measured with a load of 200 g. The microhardness shows no significant change with a load exceeding 500 g. This kind of behaviour is also observed in the Zr based bulk amorphous alloys.

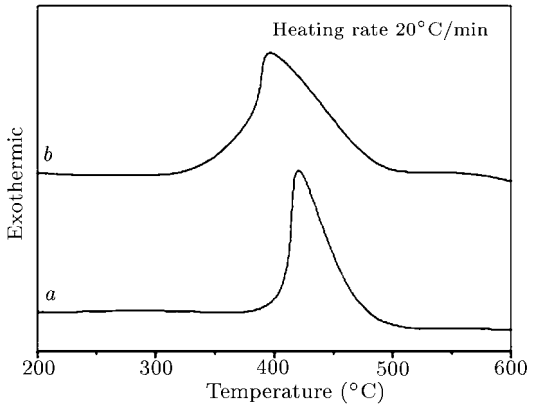

Fig. 6. DSC curves of $Mg_{55}Ni_{35}Si_{10}$ for (a) the 68-h as-milled and (b) bulk specimen.

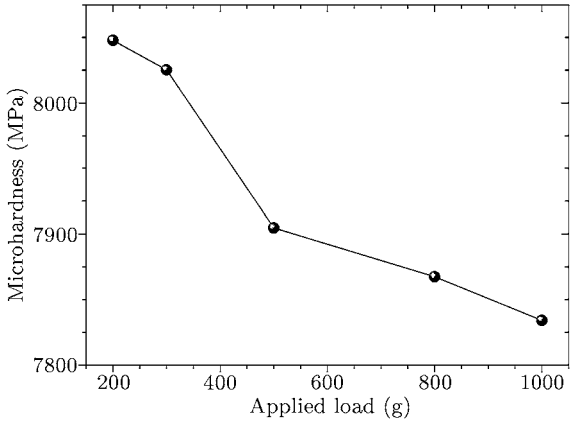

Fig. 7. The Vickers microhardnesses of the bulk $Mg_{55}Ni_{35}Si_{10}$ amorphous specimen.

The bending strength and compressive strength of $Mg_{55}Ni_{35}Si_{10}$ are 529 MPa and 1466 MPa, respectively. The fractography of the amorphous $Mg_{55}Ni_{35}Si_{10}$ bulk specimen after compressive test is present in Fig. 8. It can be seen that a large number of pores obviously exist in the bulk sample and the fracture surface is of cleavage type. The density of the hot pressed sample is 5.287 g/cm^3, which is 95.6% of the theoretical density, indicating that the consolidation parameters in our current study are not fully optimized.

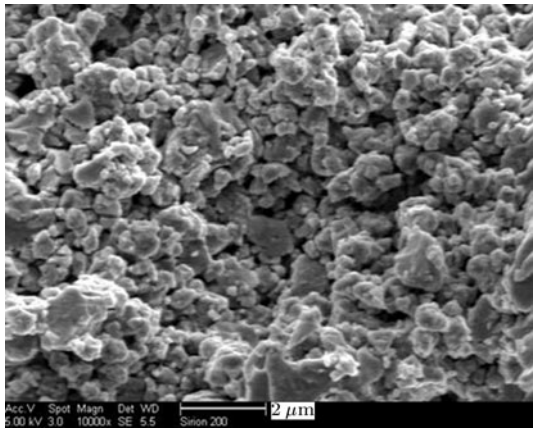

Fig. 8. The fractography of the amorphous $Mg_{55}Ni_{35}Si_{10}$ bulk specimen after compressive test.

In summary, we have fabricated amorphous $Mg_{55}Ni_{35}Si_{10}$ powders by milling elemental powder mixtures for 68 h. The amorphous powders are found to exhibit a relatively high crystallization temperature of 380° C. The as-milled amorphous $Mg_{55}Ni_{35}Si_{10}$ powders are consolidated successfully into bulk body by a vacuum hot pressing technique. Limited nanocrystallization is noticed such that the thermal stability of bulk sample is lower than the as-milled powders. The Vickers microhardness of the $Mg_{55}Ni_{35}Si_{10}$ bulk sample is in the range from 7834 to 8048 MPa. Its bending strength and compressive strength are 529 MPa and 1466 MPa, respectively.

References

[1] Song G L and Atrens A 2003 *Adv. Eng. Mater.* **5** 837
[2] Mordike B L 2001 *J. Mater. Proc. Tech.* **117** 391
[3] Watanabe H, Mukai T, Mabuchi M and Higashi K 2001 *Acta Mater.* **49** 2027
[4] Tang M B, Zhao D Q, Pan M X and Wang W H 2004 *Chin. Phys. Lett.* **21** 901
[5] Seidel M, Echkert J, Zueco-Rodrigo E and Schultz L 1996 *J. Non-Cryst. Solids.* **205-207** 514
[6] Schlorke N, Weiss B, Echert J and Schultz L 1999 *Nanostruct. Mater.* **12** 127
[7] Gennari F C, Urretavizcaya G, Andrade Gamboa J J and Meyer G 2003 *J. Alloys. Comp.* **354** 187
[8] Su S Y, He Y, Shiflet G J, Poon S J 1994 *Mater. Sci. Eng.* A. **185** 115
[9] Soifer Y M, Kobelev N P, Brodova I G., Manukhin A N, Korin E and Soifer L 1999 *Nanostruct. Mater.* **12** 875
[10] Ozaki K, Kobayashi K, Sugiyama A, Nishio T and Matsumoto A 2000 *J. Powd. Metall.* **47** 423
[11] Hazelton L E, Nielsen C A, Deshmukh U V, Pierini P E 1990 *Structural Applications of Mechanical Alloying* ed Froes F H, de Barbadillo J J (Materials Park, OH: ASM International)
[12] Huang J Y, Ye L L, Wu Y K and Ye H Q 1996 *Acta Mater.* **44** 1781
[13] Sargent P M 1986 *Microindentation Techniques in Materials Sciences and Engineering* ed Blau P J, Lawn B R (Philadelphia: ASTM) p 160
[14] Mott B W 1956 Microindentation Hardness Testing (London: Butterworths)